Bulletin of Earth Sciences of Thailand

Petrochemistry of granite from Takua Pit Thong area, Ratchaburi, Thailand

Karn Phountong[1], Abhisit Salam[1*], and Takayuki Manaka[2]

1. Department of Geology, Faculty of Science, Chulalongkorn University, Bangkok 10330, Thailand
2. Mineral Resources Research Group, Research Institute for Geo-Resources and Environment, Geological Survey of Japan (AIST), Tsukuba, Ibaraki 305-8567, Japan
*Corresponding author email: Abhisit.S@gmail.com

ABSTRACT

Takua Pit Thong mine was a tin-tungsten mine associated with granites of the Western Granite Belt. Petrographic and geochemical studies reveal two granitic rock units: porphyritic granite and equigranular granite. Both granites show similar petrography characteristics except for tourmaline which appears only in equigranular granite, and their texture. Based on whole-rock geochemistry, porphyritic granite is ferroan, alkalic, peraluminous monzonite whereas equigranular granite is ferroan, alkali- to alkali-calcic, peraluminous granodiorite. Both granites show S-type affinity. Trace element plots, i.e. Rb-Y-Nb and Rb-Yb-Ta space, classify both granites to syn-collisional and within-plate granites. Moreover, the enrichment in LILE (e.g. K, Rb) and HFSE (e.g. Nb, Ti) support that the both granites formed by the partial melting of sedimentary rock in a post-collisional setting.

Keywords: Granite, Geochemistry, Thailand, Southeast Asian Tin Belt

1. Introduction

The Southeast Asian Tin Belt is one of the biggest tin-tungsten producing areas of the world. Before the tin price crisis, it was accounted for 54% of the world's tin production (Schwartz et al., 1995). The belt is almost a north-south trend, from East Myanmar, Thailand, Peninsular Malaysia, and Indonesia's Belitung (Cobbing et al., 1986; Cobbing et al., 1992). In the north, the belt may extend to Yunnan in Southern China. In recent years, Thailand still produces small amount of tin accounting for 341 metric tons of the world's tin production (Reichl and Schatz, 2019). Myanmar still remain one of major producing tin and tungsten regions and was ranked to the 3rd world's tin production with 67,300 metric tons or 22.36% of all tin production in 2017 (Reichl and Schatz, 2019). The other top 2 tin producing countries in 2017 were China, which produced 74,800 metric tons or 24.85% of world's tin production, and Indonesia, which produced 68,702 metric tons or 22.83% of world's tin production (Reichl and Schatz, 2019).

The study area which includes Takua Pit Thong Tin-Tungsten Deposit is in Suan Phueng District, Ratchaburi Province, western Thailand (Figure 1), approximately 200 km west of Bangkok. The Takua Pit Thong mine used to be operated during tin-tungsten booming time (Mahawat, 1988). The deposit was classified as contact metasomatic tin deposit (Hosking, 1988) or skarn type deposit. Mineralization formed between Upper Cretaceous granite and Ordovician limestone host rock (Suvansavate, 1986; Mahawat, 1988).

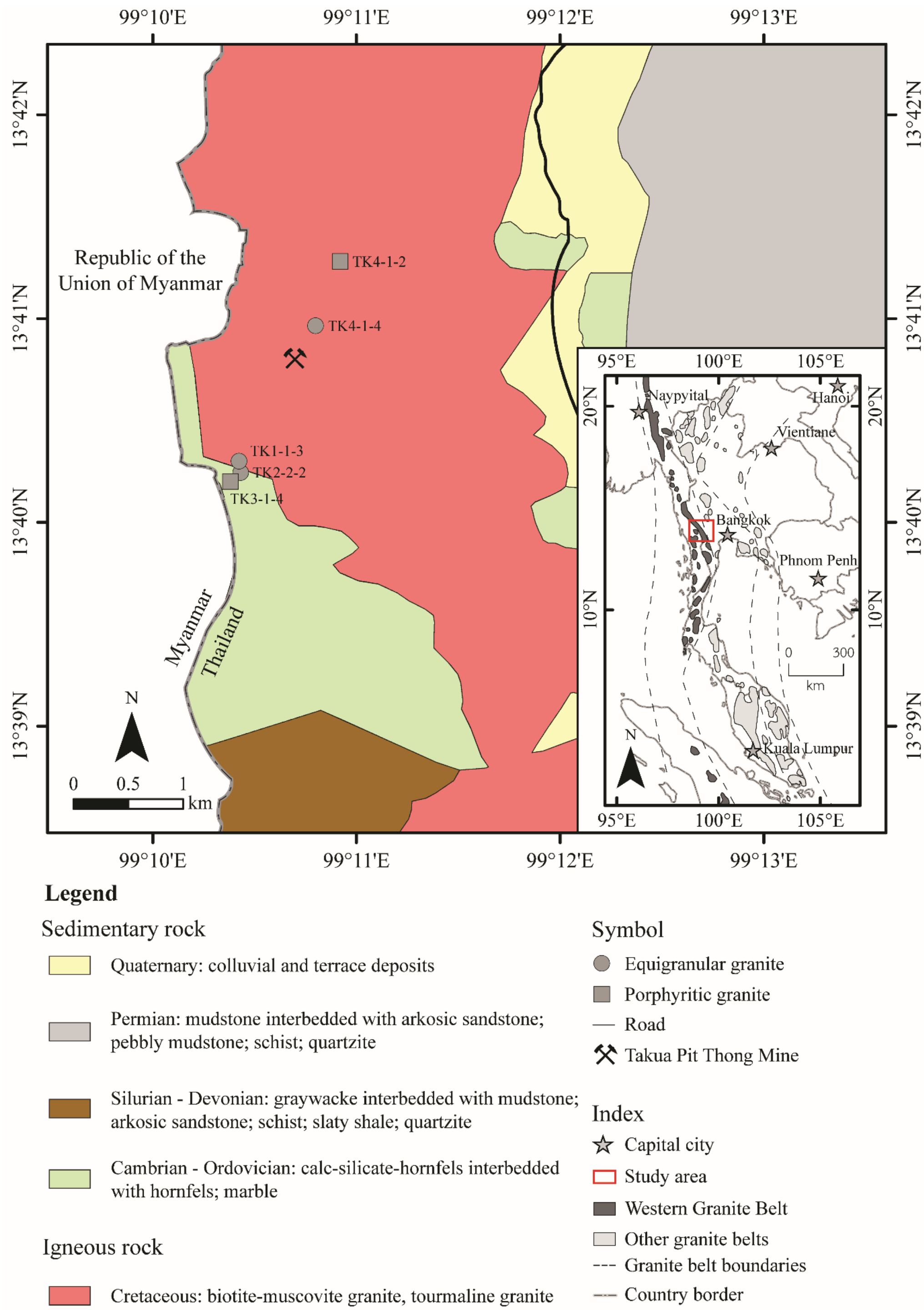

Figure 1 Geological map of the Takua Pit Thong area, Ratchaburi Province, western Thailand (modified after Dheeradilok et al., 1985; Leewongcharoen and Chaturongkawanich, 1994) and samples location. Index map shows granitoids emplacement and their boundaries (modified after Charusiri et al., 1993)

Prior to this study, some petrographic and mineralization studies have been undertaken in the area. However, the geochemistry of granitic rocks has never been carried out. This study focuses on granitic rocks in the mine and its adjacent area to determine geological and geochemical characteristics of granites for implication of their tectonic setting.

2. Geological Setting

Thailand lies within two main tectonic blocks, from west to east: Shan-Thai (SIBUMASU) Block and Indochina Block (Bunopas, 1981; Metcalfe, 1988). In between, there are Sukhothai Fold Belt in the west (Bunopas, 1981; Metcalfe, 1988; Barr and Macdonald, 1991; Sone and Metcalfe, 2008) and Loei Fold Belt in the east (Bunopas, 1981; Charusiri et al., 2002; Burrett et al., 2014)

Granite Belts in Thailand are north-south trend, and partly overlapped with the Southeast Asian Tin Belt, particularly the western tin belt. Based on their petrochemistry and geochronology, three belts have been established namely, Eastern Granite Belt, Central Granite Belt, and Western Granite Belt (Charusiri et al., 1993; Schwartz et al., 1995; Cobbing, 2011). The Western Granite, hornblende-biotite granite and biotite granite, has Upper Cretaceous to Eocene (90-50 Ma) age, both I- and S-type granite (Cobbing et al., 1986; Charusiri et al., 1993; Searle et al., 2007). It covers area between Three Pagoda Fault in the north and Khlong Marui fault in the south (Linnen, 1998). The Western Granite Belt formed as a result of the collision between Western Burma Block in the west and Sibumasu Block in the east (Charusiri et al., 1993).

Country rocks in Takua Pit Thong Deposit are Khao Noi Sethi Formation and Kanchanaburi Group (Suvansavate, 1986). Khao Noi Sethi Formation are Ordovician in age and comprised of gray marble and gray to dark gray, thin-bedded limestone intercalated with argillite and fairly well-developed minor drag fold on thin layers (Dheeradilok et al., 1985). Rocks of Kanchanaburi Group are Silurian-Devonian brown to yellowish brown quartzite and brown to greenish gray phyllite (Dheeradilok et al., 1985)

3. Methodology

The study area was explored by foot across the map from the main road to the west. Due to the complicated morphology and highly weathered condition of the outcrop, only a few representative samples from each outcrop were obtained, i.e. two samples of porphyritic granite, and three samples of equigranular granite (Figure 1). As for laboratory studies, there are three analyses in this work: petrography, major and minor oxides analysis, and trace element analysis. The first two studies were performed at Department of Geology, Faculty of Science, Chulalongkorn University, whereas four samples of trace elements, were analyzed by ALS Limited using ME-MS81™ method.

3.1. Petrography

Representative samples were prepared for rock slabs and thin sections. Then, NIKON polarizing microscope was used to observe the mineral compositions and their texture

3.2. Whole-rock Geochemistry

Unweathered samples were crushed by a jaw crusher and then were milled by Rocklabs tungsten carbide disc mill until sample's particle size is clay-size powder. These rock powder samples were separated for major and minor oxides analysis using Wavelength Dispersive X-ray Fluorescence spectrometer (WD-XRF), and for trace element analysis by ALS Limited using Inductively Couple Plasma Mass Spectrometer (ICP-MS). For XRF calibration, rock standards from Geological Survey of Japan (GSJ), i.e. JG-2, JG-1a, JB-1b, and JCFA-1, and United States Geological Survey (USGS), i.e. RGM-1, GSP-2, AGV-2, BHVO-2, were analyzed together with the samples under the same condition. All powder samples were mix with waxes with a ratio of 8:1 and were pressed into pellets prior to the analysis by BRUKER XRF model AXS S4 PIONEER, where ten major and minor oxides (i.e. SiO_2, TiO_2, Al_2O_3, FeO_{total}, MnO, MgO, CaO, Na_2O, K_2O and P_2O_5) were measure. The lower detection limit (LLD) of XRF is approximately 80 – 100 ppm for SiO_2 and Al_2O_3, 25 – 30 ppm for Na2O and MgO, and 2 – 10 ppm for other oxides. In addition, loss on ignition (LOI) were analyzed by weighing rock powder samples before and after heating at 1000° C for 1 hour, as suggested by Lechler and Desilets (1987). Data and diagrams were processed and created by GCDkit software of Janoušek et al. (2006).

4. Results

This study divided results into two sections: field observation and petrographic description; and whole-rock geochemistry.

4.1. Field observation and petrographic description

In the western part of Thailand, exposures of fresh granitic rocks are quite limited due to thick vegetation and soil covers. However, some fresh rocks were found and it was revealed that there are two types of granitic rocks based on the texture, namely 1) porphyritic granite, and 2) equigranular granite (Figure 2). In addition, some granites in the area have been altered to greisen and thus these rocks were not focused in this study. According to the petrographic study (Figure 3.) and plutonic rock modal classification (Figure 4) (after Streckeisen, 1974), porphyritic granite and equigranular granite are alkali-feldspar granite and syenogranite, respectively.

4.1.1. Porphyritic granite

Porphyritic granites are mainly found in the abandoned Takua Pit Thong mine. They are typically characterized by porphyritic texture with most of K-feldspar phenocryst (Figure 3b). The petrographic study shows that it is composed mainly of orthoclase (61 vol.%), quartz (33 vol.%), and plagioclase (6 vol.%). Accessory minerals are apatite, zircon with some opaque minerals. Quartz occurs as anhedral, fine-grained ranging in size from 0.1 – 0.5 mm. It shows equigranular texture in matrix and associated with muscovite, and biotite. Orthoclase and plagioclase form as medium-grained (2 – 5 mm), subhedral crystals and shows hiatal porphyritic texture with quartz, muscovite, and biotite. In addition, orthoclase commonly shows perthitic texture.

4.1.2. Equigranular granite

Equigranular granites expose at the margin of the abandoned mine and cover an area of 1-2 sq. km. The rocks are characterized by fine-grained, equigranular texture with some tourmaline in some parts (Figure 3c-f). The petrographic study results show that they are composed mainly of orthoclase (39 – 52 vol.%), quartz (34 – 35 vol.%), plagioclase (9 – 17 vol.%), muscovite (0 – 8 vol.%), and biotite (0 – 2 vol.%). Accessory minerals are microcline, zircon with some opaque minerals. Texturally, it is equigranular and occasionally appeared seriate porphyry. Quartz forms as fine-grained (0.25 – 0.5 mm), anhedral crystals. It shows equigranular texture in association with muscovite and biotite. Orthoclase and plagioclase occurring as fine- to medium-grained (0.5 – 2 mm), are found as subhedral crystals and show seriate porphyritic texture with quartz, muscovite, and biotite. Orthoclase also shows perthitic texture. Tourmaline minerals are found in some samples, and range in size from 1 mm to 4 mm with subhedral to anhedral shape.

4.2. Whole-rock geochemistry

Major and minor oxide results of porphyritic granite and equigranular granite are shown in Table 1, whereas trace element results are shown in Table 2. Both porphyritic granite and equigranular granite show similar CaO composition, ranging from 0.18 to 0.67 wt.%. In addition, porphyritic granite has higher Al_2O_3 and FeO_{tot}, MgO, and K_2O contents, ranging from 16.34 to 17.42 wt.%, 1.21 to 1.40 wt.%, 0.25 wt.%, and 4.25 to 4.35 wt.%, respectively, compared to equigranular granite, ranging from 13.67 to 15.58 wt.%, 0.50 to 1.24 wt.%, 0.00 to 0.17 wt.%, and 2.26 to 5.12 wt.%, respectively. In contrast, porphyritic granite shows slightly lower SiO_2 and Na_2O values, ranging from 60.15 to 60.85 wt.%, and 2.67 to 2.95 wt.%, respectively, than equigranular granite which is ranged from 67.72 to 68.82 wt.% and 2.53 to 4.00 wt.%, respectively. These major oxides are consistent with mineral assemblages of each granite, e.g. K-feldspar, plagioclase, biotite, muscovite, and tourmaline.

According to the plot of SiO_2 and alkalic content (Na_2O + K_2O) in TAS diagram (after Middlemost, 1994) (Figure 5), porphyritic granites and equigranular granites were classified as monzonite and granodiorite, respectively. Furthermore, a three-tiered classification scheme for granitic rock (after Frost et al., 2001), i.e. Fe* $[FeO_{tot}/(FeO_{tot} + MgO)]$, modified alkaline-lime index (MALI) and aluminum saturation index (ASI), were used to classify granites in this study (Figure 6).

Figure 2 Exposure of various granitic rocks in the area: (a) porphyritic granite and (b) equigranular granite.

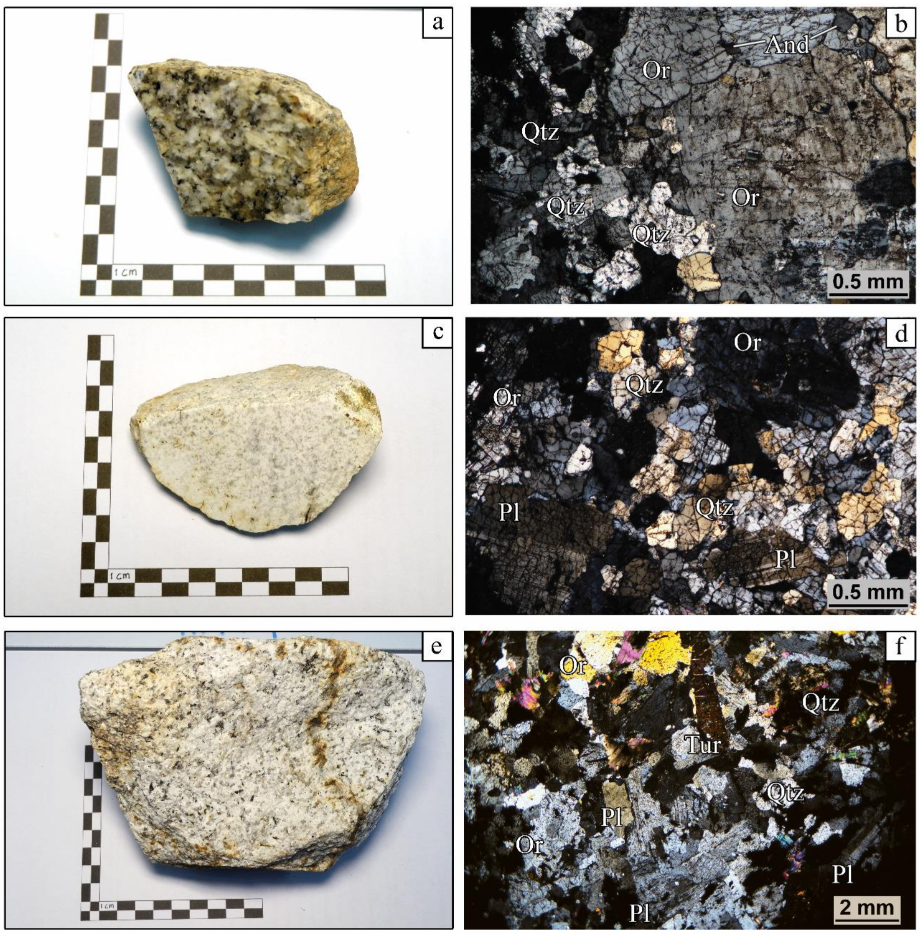

Figure 3 Hand specimens and photomicrographs under cross polarized light (XPL) showing mineral assemblages and textures: (a) and (b) porphyritic granite; (c) and (d) equigranular granite; (e) and (f) equigranular granite with distinct patchy tourmalines. Mineral abbreviations: Qtz = Quartz, Or = Orthoclase, Pl = Plagioclase, Ms = Muscovite, And = Andalusite, Tur = Tourmaline

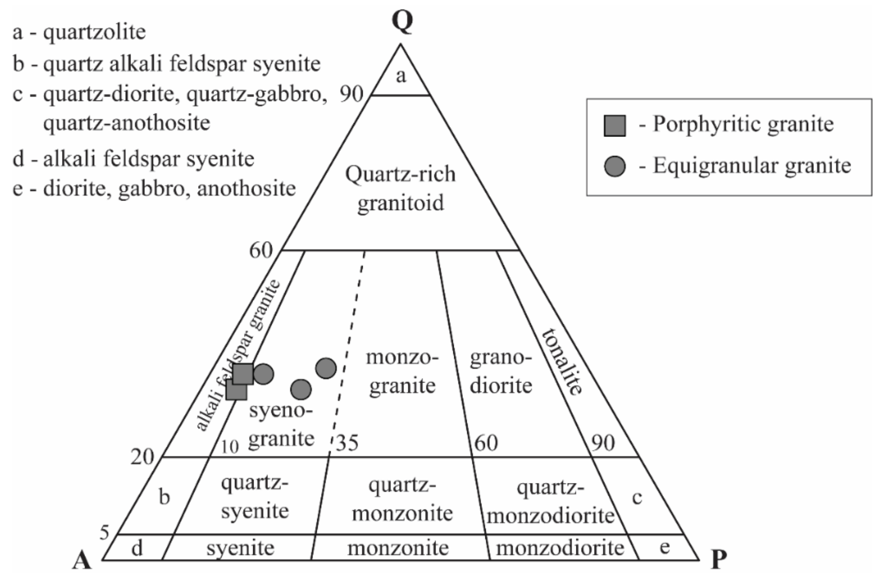

Figure 4 Modal QAP diagram (after Streckeisen, 1974) of granitic rocks in the area. Abbreviations are Q = modal quartz, A = modal alkali feldspar, P = modal plagioclase

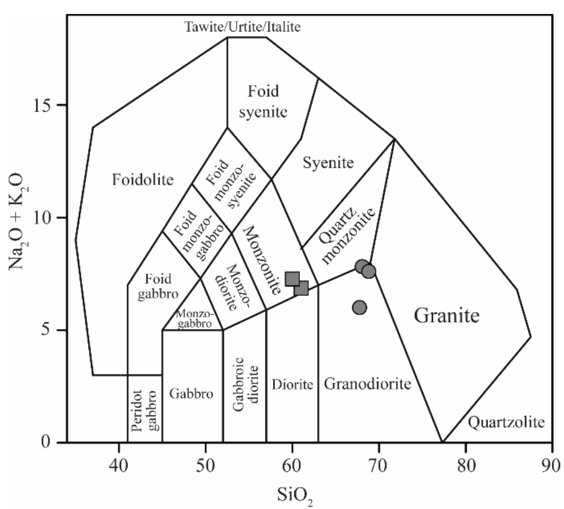

Figure 5 TAS diagram (after Middlemost, 1994) of granitic rocks in the area, plotting SiO_2 versus Na_2O+K_2O to discriminate granitoids (rock type symbols are same as Figure 4

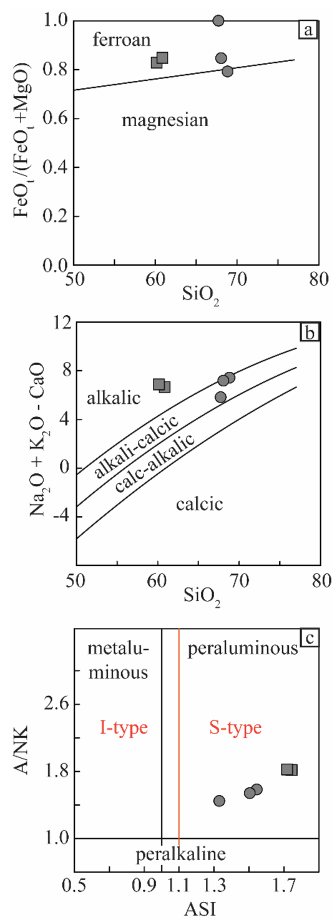

Figure 6 (right) Granitic rock discrimination diagram (after Frost et al., 2001) showing three-tiered classification scheme: (a) SiO_2 vs. Fe*; (b) SiO_2 vs. MALI; and (c) ASI vs. A/NK. Rock type symbols are same as Figure 4

Table 1 Representative major and minor oxides of granites in Takua Pit Thong area (in wt.%).

Rock Type	Porphyritic granite		Equigranular granite		
Sample No.	TK3-1-4	TK4-1-2	TK1-1-3	TK2-2-2	TK4-1-4
Major and minor oxides (wt.%)					
SiO_2	60.85	60.15	67.72	68.82	68.05
Al_2O_3	16.34	17.42	13.67	14.98	15.58
FeO_{tot}	1.40	1.21	1.24	0.65	0.50
CaO	0.26	0.42	0.18	0.22	0.67
MgO	0.25	0.25	0.00	0.17	0.09
Na_2O	2.67	2.95	3.75	2.53	4.00
K_2O	4.25	4.35	2.26	5.12	3.86
P_2O_5	0.04	0.08	0.04	0.06	0.11
TiO_2	0.06	0.08	0.03	0.04	0.06
MnO	0.12	0.12	0.08	0.17	0.06
LOI	4.19	3.26	0.94	5.09	0.92
Total	90.45	90.28	89.92	97.84	93.90

Table 2 Representative trace elements and REE of granites in Takua Pit Thong area (in ppm)

Rock Type	Porphyritic granite		Equigranular granite	
Sample No.	TK3-1-4	TK4-1-2	TK1-1-3	TK4-1-4
Trace element and REE (ppm)				
V	2.5	6	2.5	2.5
Cr	250	130	20	150
Ga	43.2	35.5	31.2	29.2
Rb	1070	801	612	646
Sr	14.4	24.8	14.5	27.7
Y	13.2	9	14.2	23.3
Zr	57	36	30	93
Nb	109	73.4	73.5	42.6
Sn	243	159	58	54
Cs	49.6	35.1	37.6	63.1
Ba	49.9	94.5	26.2	95.8
La	6.7	6.3	8.9	25.6
Ce	14.1	13.7	19	57.5
Pr	1.56	1.45	2.14	6.08
Nd	6.1	5.3	7	21.7
Sm	1.57	1.26	1.72	4.83
Eu	0.14	0.14	0.13	0.23
Gd	1.6	1.33	1.49	4.05
Tb	0.32	0.23	0.34	0.7
Dy	1.92	1.4	1.97	3.78
Ho	0.39	0.27	0.37	0.69
Er	1.3	0.81	1.16	1.87
Tm	0.22	0.13	0.22	0.29
Yb	1.57	0.92	1.54	1.82
Lu	0.24	0.15	0.23	0.27
Hf	3	1.3	1.5	3.5
Ta	33	19	29	10.2
W	21	23	12	11
Pb	38	39	29	41
Th	8.74	6.86	13.15	30.2
U	4.88	4.85	35.5	23

Moreover, plots of SiO_2 versus FeO/(FeO+MgO) (Figure 6a) show that both granites are classified as ferroan rocks, except for one plot of equigranular granite, which indicates that Fe is molecularly more abundant than Mg. However, magnesian granite was plotted very near to the boundary between ferroan and magnesian rock. As a result, the granite was considered ferroan rock. In addition, SiO_2 versus MALI (Na_2O + K_2O – CaO) diagram (Figure 6b) shows that porphyritic granite is grouped as an alkalic rock which represents more abundance of alkali content than CaO. In contrast, equigranular granite is classified to be alkali-calcic rock which represents lower alkali content compared to CaO. Moreover, ASI diagram, the molecular Al(Na + K) vs. Al/(Ca – 1.67P + Na + K) (Figure 6c), shows that both granites are peraluminous granite which suggests high aluminum content compared to alkali content and thus they are indicated to be S-type granite (Figure 6c). Moreover, the scattered distribution in Harker variation diagrams (Figure 7) can support the S-type granite character.

The primitive mantle-normalized (value from Sun and McDonough, 1989) spider diagrams (Figure 8a, c) showing the enrichment of U and Pb can only imply that it might be related to felsic magma and can be consistent with the U-Pb bearing minerals, e.g. monazite, xenotime, apatite, zircon. In addition, there are enrichment of Cs, Rb and K which are large ion lithophile elements (LILE), and enrichment of some high field strength elements (HFSE; e.g. Zr, Ti). The chondrite-normalized (values from Boynton, 1984) REE patterns (Figure 8b, d) show that both granites have slightly higher Light-REE (LREE) than Heavy-REE (HREE).

5. Discussion

Results from the previous section can be discussed in term of petrogenesis of the granitic rock and implication for geotectonic environment for the study area.

5.1. Petrogenesis

From the field observation and the petrographic study, the two types of granites have felsic composition. ASI index values indicate that all rocks are peraluminous and S-type affinity and it is suggested that the both granites are of sedimentary rock in origin, which is agreed with some previous work in the same granitoid belt (e.g. Charusiri et al., 1993; Cobbing, 2011). Their mineral assemblages, particularly muscovite and tourmaline, support the genetic model of sedimentary partial melting as the both minerals commonly have high Al contents. Moreover, the whole-rock trace elements composition shows relatively high Th and U, which are typical for felsic magma derivation. Enrichment of LILE suggests that magma evolution of both granites is in the late stage. Moreover, slightly high LREE/HREE reflects the low degree of partial melting

Trace elements plots of Y+Nb vs. Rb (Figure 9a) indicate that both granites are plotted on syn-collision granite (syn-COLG) field, whereas plots of Y vs. Nb and Yb vs. Ta (Figure 9b-c) show that both granites are within plate granite (WPG). In addition, plots between Ta+Yb and Rb (Figure 9d) shows result ranging from syn-COLG to WPG. These wide range plots, but do not show any orogenic granite (ORG), together with their S-type affinity, and enrichment of LILE and HFSE, suggest that both granites are post-collision granite which formed by both melting of the lower crust and melting of the upper mantle (Pearce et al., 1984; Pearce, 1996).

5.2. Tectonic Implication

The petrogenetic condition of granites in Takua Pit Thong area is suggested to be anatexis of sedimentary rocks. Although geochronology is not directly carried out in this study to interpret the timing of tectonic event, using geotectonic assumption from previous studies (e.g. Bunopas, 1981; Bunopas and Vella, 1983; Cobbing et al., 1986; Charusiri et al., 1993; Schwartz et al., 1995; Charusiri et al., 2002; Cobbing, 2011; Zaw et al., 2014), and the location of the mine which is located at the margin between Sibumasu block and Western Burma block, can be inferred that both granites were resulted from the compressional condition from the collision between these two blocks.

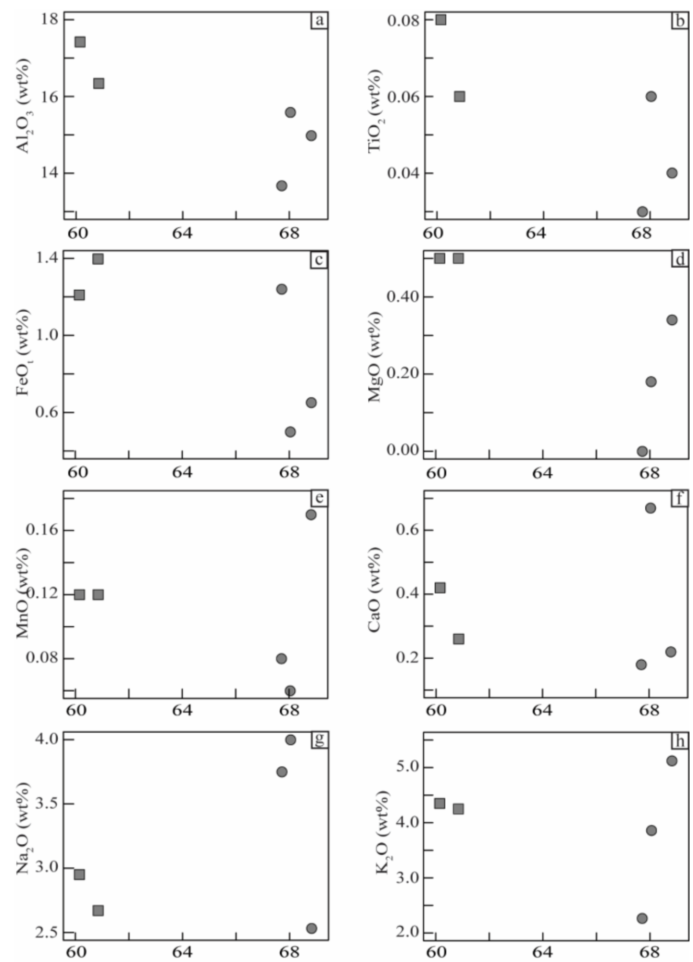

Figure 7 Harker variation diagrams (Harker, 1909) plotting SiO_2 against major and minor oxides (rock type symbols are same as Figure 4)

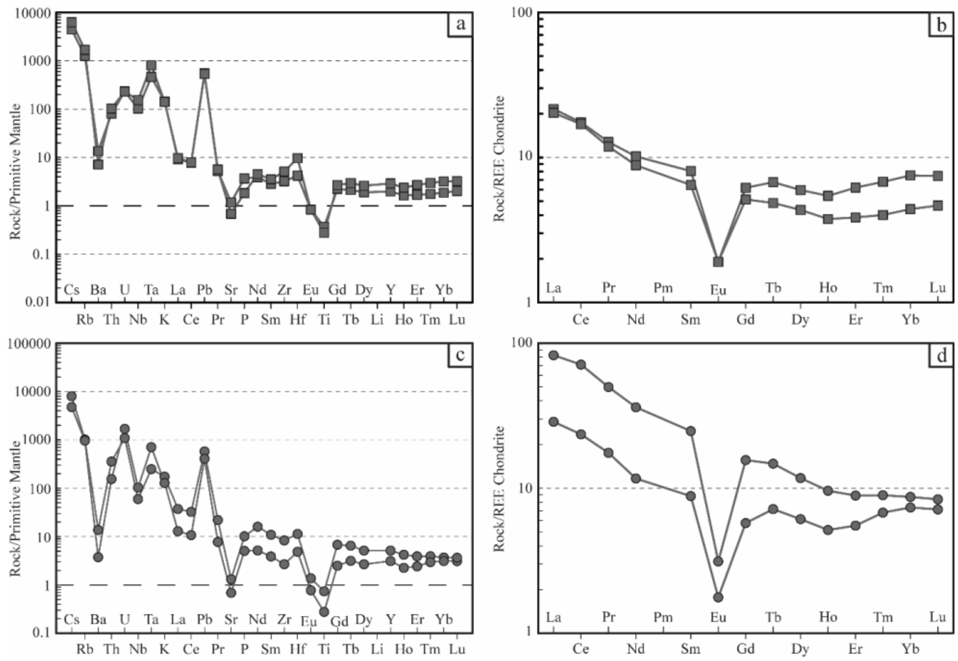

Figure 8 Normalized spider diagrams showing REE and other trace elements pattern of granites in the area: (a, c) primitive mantle-normalized (value from Sun and McDonough, 1989) spider diagrams; (b, d) chondrite-normalized (value from Boynton, 1984) REE pattern. Rock type symbols are same as Figure 4

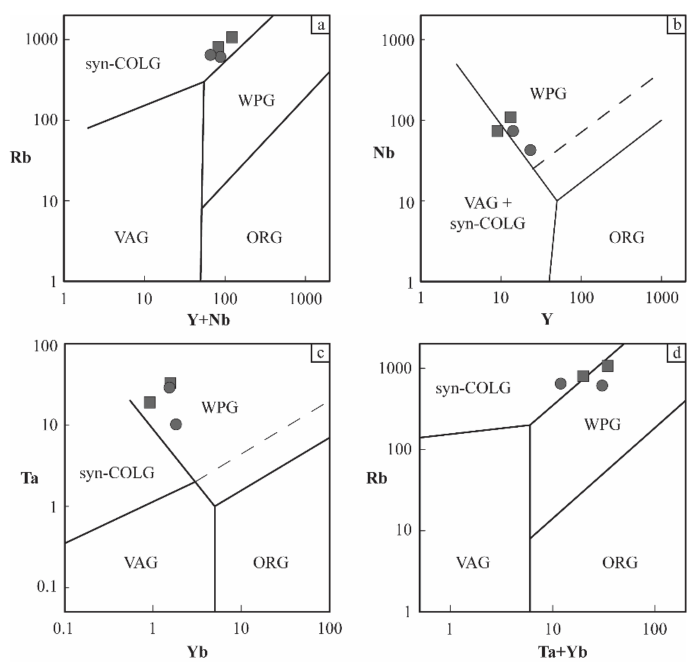

Figure 9 Immobile elements plots of granites in the area: (a) Y+Nb vs. Rb; (b) Y vs. Nb; (c) Yb vs. Ta; (d) Ta+Yb vs. Rb. Rock type symbols are same as Figure 4

6. Conclusion

Studies on petrology and whole-rock geochemistry of granitic rocks from the Takua Pit Thong area, western Thailand concluded a few key points which are summarized below.

(1) There are two units of granitic rock: porphyritic granite, and equigranular granite, which are differentiated using petrography and whole-rock geochemistry.

(2) Porphyritic granite is ferroan, alkalic, peraluminous rock, whereas equigranular granite is ferroan, alkali-calcic, peraluminous rock. Both granites indicate S-type granite affinity.

(3) Geochemical characters, together with enrichment of LILE and HFSE, suggest that both granites were resulted from post-collisional felsic magma.

Acknowledgement

We would like to thank Department of Geology, Faculty of science, Chulalongkorn University for laboratory analysis. In addition, this research is supported by Graduate School Thesis Grant, Chulalongkorn University.

References

Barr, S. M., and Macdonald, A. S. 1991. Toward a late Palaeozoic-early Mesozoic tectonic model for Thailand. *Journal of Thai Geosciences*, 1, 11-22.

Boynton, W. V. 1984. Cosmochemistry of the rare earth elements: meteorite studies. In P. Henderson (ed.), *Rare Earth Element Geochemistry*, vol. 2. Developments in Geochemistry. pp. 63-114. Amsterdam: Elsevier.

Bunopas, S. 1981. Paleogeographic history of Western Thailand and adjacent parts of South-east Asia. Unpublished Doctoral dissertation. Victoria University of Wellington.

Bunopas, S., and Vella, P. 1983. Tectonic and geologic evolution of Thailand. In P. Nutalaya (ed.), *Proceedings of a workshop on stratigraphic correlation of Thailand and Malaysia*, Bangkok, pp. 307-322.

Burrett, C., Zaw, K., Meffre, S., Lai, C. K., Khositanont, S., Chaodumrong, P., Udchachon, M., Ekins, S., and Halpin, J. 2014. The configuration of Greater Gondwana—Evidence from LA ICPMS, U–Pb geochronology of detrital zircons from the Palaeozoic and Mesozoic of Southeast Asia and China. *Gondwana Research*, 26, 31-51.

Charusiri, P., Clark, A. H., Farrar, E., Archibald, D., and Charusiri, B. 1993. Granite belts in Thailand: evidence from the $^{40}Ar/^{39}Ar$ geochronological and geological syntheses. *Journal of Southeast Asian Earth Sciences*, 8, 1, 127-136.

Charusiri, P., Daorerk, V., Archibald, D., Hisada, K., and Ampaiwan, T. 2002. Geotectonic Evolution of Thailand : A New Synthesis. *Journal of Geological Society of Thailand*, 1, 1-20.

Cobbing, E. J. 2011. Granitic rocks. In M. F. Ridd, A. J. Barber, and M. J. Crow (eds.), *The Geology of*

Thailand, pp. 441-458. London: Geological Society.

Cobbing, E. J., Mallick, D. I. J., Pitfield, P. E. J., and Teoh, L. H. 1986. The granites of the Southeast Asian Tin Belt. *Journal of the Geological Society*, 143, 3, 537-550.

Cobbing, E. J., Pitfield, P. E. J., Derbyshire, D. P. F., and Mallick, D. I. J. 1992. *The granites of the South-East Asian tin belt*. vol. 10. Overseas Memoir of the British Geological Survey. London: British Geological Survey.

Dheeradilok, P., Udomsrisuk, T., Tansuwan, V., Jungyusuk, N., and Nakanart, A. 1985. *Changwat Nakhorn Pathom*[Geological map]. Sheet ND47-11, Scale 1:250,000. Bangkok: Department of Mineral Resources.

Frost, B. R., Barnes, C. G., Collins, W. J., Arculus, R. J., Ellis, D. J., and Frost, C. D. 2001. A geochemical classification for granitic rocks. *Journal of petrology*, 42, 11, 2033-2048.

Hosking, K. F. G. 1988. The world's major types of tin deposit. In C. S. Hutchison (ed.), *Geology of Tin Deposits in Asia and the Pacific*, pp. 3-49. Berlin: Springer-Verlag.

Janoušek, V., Farrow, C. M., and Erban, V. 2006. Interpretation of Whole-rock Geochemical Data in Igneous Geochemistry: Introducing Geochemical Data Toolkit (GCDkit). *Journal of Petrology*, 47, 6, 1255-1259.

Lechler, P. J., and Desilets, M. O. 1987. A review of the use of loss on ignition as a measurement of total volatiles in whole-rock analysis. *Chemical Geology*, 63, 3, 341-344.

Leewongcharoen, S., and Chaturongkawanich, S. 1994. *Muang Thung Chedi Quadrangle*[Geological map]. Sheet 4836III, Scale 1:50,000. Bangkok: Department of Mineral Resources,.

Linnen, R. L. 1998. Depth of emplacement, fluid provenance and metallogeny in granitic terranes: a comparison of western Thailand with other tin belts. *Mineralium Deposita*, 33, 5, 461-476.

Mahawat, C. 1988. The geological characteristics of the Pilok Sn-W-Mo deposits, west Thailand. In C. S. Hutchison (ed.), *Geology of Tin Deposits in Asia and the Pacific*, New York, pp. 696-709.

Metcalfe, I. 1988. Origin and assembly of south-east Asian continental terranes. In M. G. Audley-Charles, and A. Hallam (eds.), *Gondwana and Tethys*, vol. 37. Geological Society Special Publications. pp. 101-118. New York: Oxford University Press.

Middlemost, E. A. K. 1994. Naming materials in the magma/igneous rock system. *Earth-Science Reviews*, 37, 3, 215-224.

Pearce, J. A. 1996. Sources and settings of granitic rocks. *Episodes*, 19, 120-125.

Pearce, J. A., Harris, N. B. W., and Tindle, A. G. 1984. Trace element discrimination diagrams for the tectonic interpretation of granitic rocks. *Journal of Petrology*, 25, 956-983.

Reichl, C., and Schatz, M. 2019. *World Mining Data 2019*. vol. 34. Minerals Production. Vienna: International Organizing Committee for the World Mining Congresses.

Schwartz, M. O., Rajah, S. S., Askury, A. K., Putthapiban, P., and Djaswadi, S. 1995. The Southeast Asian tin belt. *Earth-Science Reviews*, 38, 2, 95-293.

Searle, M. P., Noble, S. R., Cottle, J. M., Waters, D. J., Mitchell, A. H. G., Hlaing, T., and Horstwood, M. S. A. 2007. Tectonic evolution of the Mogok metamorphic belt, Burma (Myanmar) constrained by U-Th-Pb dating of metamorphic and magmatic rocks. *Tectonics*, 26, 3

Sone, M., and Metcalfe, I. 2008. Parallel Tethyan sutures in mainland Southeast Asia: New insights for Palaeo-Tethys closure and implications for the Indosinian orogeny. *Comptes Rendus Geoscience*, 340, 2, 166-179.

Streckeisen, A. 1974. Classification and nomenclature of plutonic rocks recommendations of the IUGS subcommission on the systematics of igneous rocks. *Geologische Rundschau*, 63, 2, 773-786.

Sun, S.-s., and McDonough, W. F. 1989. Chemical and isotopic systematics of oceanic basalts: implications for mantle composition and processes. *Geological Society, London, Special Publications*, 42, 1, 313-345.

Suvansavate, A. 1986. Geological and mineralogical studies of the cassiterite-sulfide ore deposit at the Takua Pit Thong mine, Changwat Ratchaburi. Unpublished Master's Thesis. Department of Geology, Graduate School, Chulalongkorn University.

Zaw, K., Meffre, S., Lai, C., Burrett, C., Santosh, M., Graham, I., Manaka, T., Salam, A., Kamvong, T., and Cromie, P. 2014. Tectonics and metallogeny of mainland Southeast Asia — A review and contribution. *Gondwana Research*, 26, 1, 5-30.